ACS OMEGA

http://pubs.acs.org/journal/acsodf

Article

Synthesis of Metal−Organic Frameworks MIL-101(Cr)-NH_2 Containing Phosphorous Acid Functional Groups: Application for the Synthesis of *N*-Amino-2-pyridone and Pyrano [2,3-*c*]pyrazole Derivatives via a Cooperative Vinylogous Anomeric-Based Oxidation

Saeed Babaee, Mahmoud Zarei,* Hassan Sepehrmansourie, Mohammad Ali Zolfigol,* and Sadegh Rostamnia*

Cite This: *ACS Omega* 2020, 5, 6240−6249

Read Online

ACCESS | Metrics & More | Article Recommendations | Supporting Information

ABSTRACT: In the current paper, we successfully developed and used metal−organic frameworks (MOFs) based on MIL-101(Cr)-NH_2 with phosphorus acid functional groups MIL-101(Cr)-$N(CH_2PO_3H_2)_2$. The synthesized metal−organic frameworks (MOFs) as a multi-functional heterogeneous and nanoporous catalyst were used for the synthesis of *N*-amino-2-pyridone and pyrano [2,3-*c*]pyrazole derivatives via reaction of ethyl cyanoacetate or ethyl acetoacetate, hydrazine hydrate, malononitrile, and various aldehydes. The final step of the reaction mechanism was preceded by a cooperative vinylogous anomeric-based oxidation. Recycle and reusability of the described catalyst MIL-101(Cr)-$N(CH_2PO_3H_2)_2$ were also investigated.

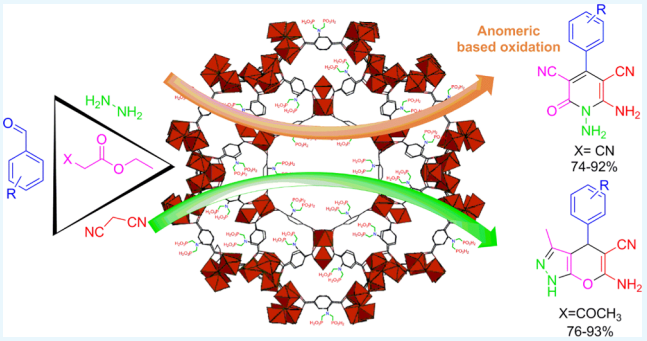

1. INTRODUCTION

Metal−organic frameworks (MOFs) have been considered as a new category of nanoporous material. They have been used for various purposes such as storage and separation of gas, catalysts, and heavy-metal adsorption.[1−5] Metal−organic frameworks (MOFs) based on the type of their ligands and functional groups on their surface exhibit different properties. Their functional groups may be initially present in the organic ligand structures or after synthesizing MOFs to create functional groups within the structure.[6] Metal−organic frameworks (MOFs) exhibit a unique catalytic role in the preparation of hydrogen and methane gas and the synthesis of a wide range of chemical and pharmaceutical compounds. These compounds have shown a unique catalytic power due to their nanosize and porous structures with various functional groups.[5,7,8] Developing Cr-based metal−organic frameworks (MOFs) is envisaged to achieve the goals such as: higher surface area, enhanced adsorption, water, and thermal stability in the course of reaction processes.[9,10]

Phosphorous acid and its derivatives are used as reagents, absorbents, catalysts for the preparation of food additives, precursor for the synthesis of phosphate fertilizers,[11] and in pharmaceutical industries due to their nontoxicity as pH regulators. The design and synthesis of catalysts with phosphorous acid moieties are an attractive research proposal due to their biocompatibility. Recently, we have reported glycoluril, MIL-100(Cr)/En, and mesoporous SBA-15 with phosphorous acid tags.[12−16] Design, synthesis, and use of metal−organic frameworks (MOFs) with phosphorous acid arms due to their properties of recovery, reuse, and high efficiency are suitable catalysts in the chemical processes.

Heterocyclic moieties have been used as important building blocks within a wide range of medicinal and biologically active molecules.[17−19] Two of the most important subclasses of heterocyclic chemistry are oxygen- and nitrogen-containing rings, which can be found in the skeletal structures of various types of biologically active and pharmaceutical compounds[20,21] (Scheme 1). Among oxygen and nitrogen hetreocycles, the *N*-amino-2-pyridones and pyrano [2,3-*c*]pyrazoles have been shown to have anticancer, anticoagulant, anticonvulsant, antimicrobial, anti-HIV, antimalarial, antitumor, antibacterial, antifungal, and antitumor properties.

In spite of large usage of *N*-amino-2-pyridones and pyrano [2,3-*c*]pyrazoles, only a few procedures have been developed for their synthesis, using piperidine, ZnO, sodium L-ascorbatea, and nano-$M^{II}Zr(PO_4)_6$ as catalysts.[22−25] Therefore, the develop-

Received: July 11, 2019
Accepted: March 5, 2020
Published: March 20, 2020

https://dx.doi.org/10.1021/acsomega.9b02133
ACS Omega 2020, 5, 6240−6249

Scheme 1. Biological Compounds Containing Heterocyclic in the Structure

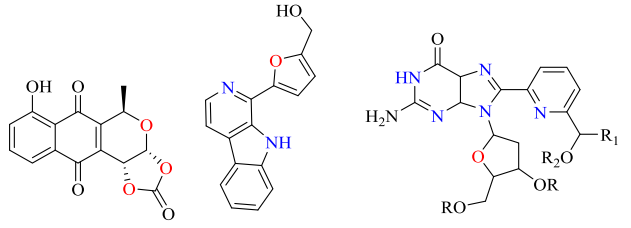

ment of new methodologies for the preparation of *N*-amino-2-pyridones and pyrano [2,3-*c*]pyrazoles is in great demand.

In the continuation of our previous investigation on the applications of catalysts with phosphorous acid functional groups, we have decided to design and synthesize a novel MIL-101(Cr)-N($CH_2PO_3H_2$)$_2$ with phosphorous acidic arms as nanoporous MOFs and heterogeneous catalyst for the one-pot synthesis of pyrano [2,3-*c*]pyrazoles and *N*-amino-2-pyridones. The desired compounds were produced through the condensation of ethyl cyanoacetate or ethyl acetoacetate, hydrazine hydrate, malononitrile, and various aldehydes via a cooperative vinylogous anomeric-based oxidation mechanism and under solvent-free conditions (Scheme 2).

Scheme 2. Synthesis of *N*-Amino-2-pyridones and Pyrano [2,3-*c*]pyrazoles in Four-Component Reaction

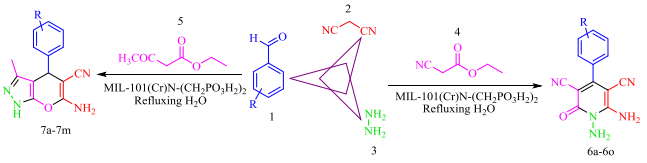

2. RESULTS AND DISCUSSION

In this paper, we reported a clean method for the preparation of MIL-101(Cr)-N($CH_2PO_3H_2$)$_2$ as a metal−organic framework (MOFs) by the one-pot reaction of MIL-101(Cr)-NH_2, formaldehyde, phosphorous acid, and *p*-toluenesulfonic acid (*p*-TSA) under refluxing EtOH. This catalyst was fully characterized by Fourier transform infrared (FT-IR), X-ray diffraction (XRD), energy-dispersive X-ray spectroscopy (EDX), elemental mapping analysis, the scanning electron microscopy (SEM), transmission electron microscopy (TEM), thermal gravimetric (TG), derivative thermal gravimetric (DTG), differential thermal analysis (DTA), and nitrogen adsorption−desorption isotherm Brunauer−Emmett−Teller (BET). Also, MIL-101(Cr)-N($CH_2PO_3H_2$)$_2$ was tested for the synthesis of *N*-amino-2-pyridone and pyrano [2,3-*c*]pyrazole derivatives.

The FT-IR spectrum of MIL-101(Cr)-NH_2 and MIL-101(Cr)-N($CH_2PO_3H_2$)$_2$ is compared in Figure 1. The broad peak at 2600−3500 cm^{-1} was related to the OH of PO_3H_2 groups. Also, the absorption bands observed at 1021 and 1081 cm^{-1} are related to the P−O bond stretching and that at 1146 cm^{-1} is related to P═O.[26] Furthermore, peaks of Cr−O of octahedral CrO_6 appeared at 1391 cm^{-1} respectively[27] (Figure 1). The FT-IR spectrum difference between MIL-101(Cr)-NH_2 and MIL-101(Cr)-N($CH_2PO_3H_2$)$_2$ confirmed the structure of the catalyst.

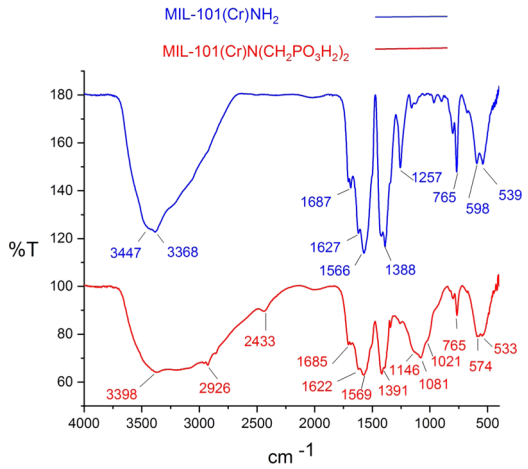

Figure 1. FT-IR spectra of MIL-101(Cr)-NH_2 and MIL-101(Cr)-N($CH_2PO_3H_2$)$_2$.

The presenting elements can be seen in the structure and morphology of MIL-101(Cr)-N($CH_2PO_3H_2$)$_2$ using energy-dispersive X-ray spectroscopy (EDX), elemental mapping analysis, and scanning electron microscopy (SEM). Through energy-dispersive X-ray spectroscopy (EDX) and elemental mapping analysis, chrome, carbon, nitrogen, oxygen, and phosphor were confirmed in the structure of MIL-101(Cr)-N($CH_2PO_3H_2$)$_2$ (Figure 2).

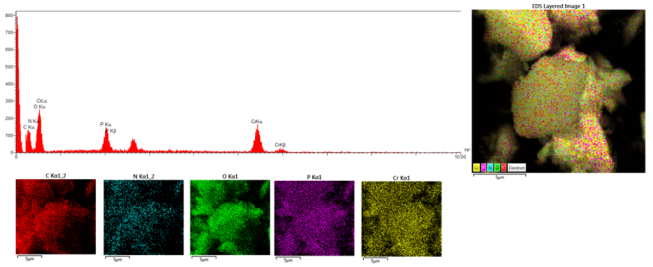

Figure 2. Energy-dispersive X-ray spectroscopy (EDX) and elemental mapping analysis of MIL-101(Cr)-N($CH_2PO_3H_2$)$_2$.

MIL-101(Cr)-NH_2 and MIL-101(Cr)-N($CH_2PO_3H_2$)$_2$ structures were calculated in the range of 2−80° using XRD as shown in Figure 3. The XRD patterns of our synthesized MIL-

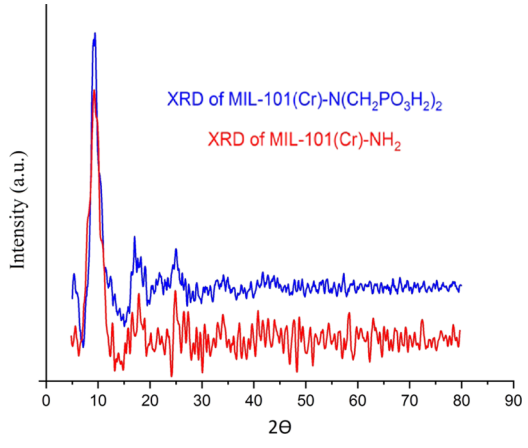

Figure 3. XRD of MIL-101(Cr)-NH_2 and MIL-101(Cr)-N($CH_2PO_3H_2$)$_2$ as MOFs catalyst.

https://dx.doi.org/10.1021/acsomega.9b02133
ACS Omega 2020, 5, 6240−6249

101(Cr)-NH_2 matched well with those reported in the literature,[28,29] confirming the formation of MIL-101(Cr)-NH_2. The main Bragg reflection around 2θ = 10 confirmed the successful synthesis of MIL-101(Cr)-NH_2 as the MOF structure. The pattern of the phosphonic acid grafted MOF materials exhibits a very similar profile to the pattern of the as-synthesized MIL-101(Cr)-NH_2 and is composed of main diffraction peaks of the MOF, confirming that the structures of MIL-101 (Cr)-NH_2 remained intact with no apparent loss of crystallinity but with some slight decrease in peak intensities along with an increase in phosphonic acid contents due to the partial filling by the grafting guest molecules.

The shape, morphology, and elements of MIL-101(Cr)-NH_2 and MIL-101(Cr)-N$(CH_2PO_3H_2)_2$ were studied using SEM analysis. SEM images of MOFs catalyst reveal that the particles are cauliflower and the particle size is within the range of the nanoscales 13.77 and 30.55 (Figures 4 and 5). Figure 6 also

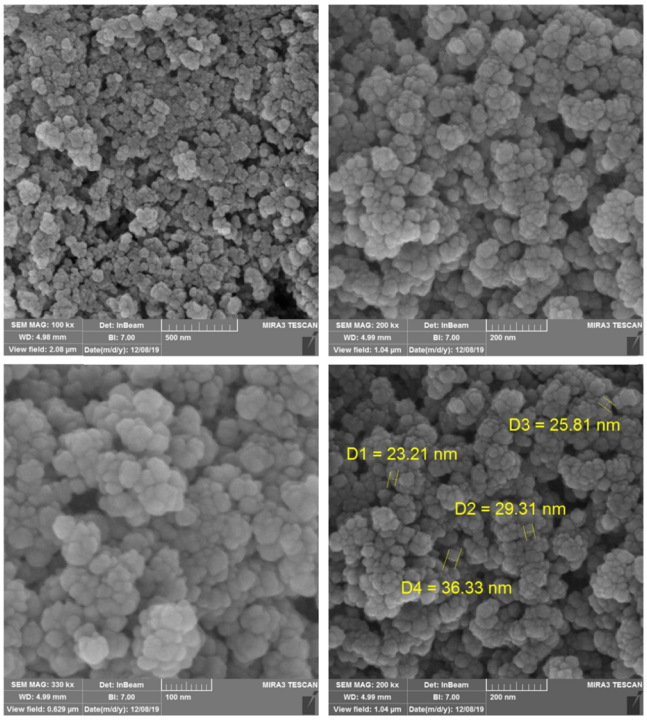

Figure 4. SEM images of MIL-101(Cr)-NH_2.

shows the results of transmission electron microscopy (TEM) images of MIL-101(Cr)-N$(CH_2PO_3H_2)_2$. Morphology and topology of MOF catalysts were confirmed to be quasi-cube structure. The particles of MIL-101(Cr)-N$(CH_2PO_3H_2)_2$ were observed to of nano size (approximately 30−40 nm) with proper dispersion.

Thermal gravimetric (TG) analysis and differential thermal analysis (DTA) of MIL-101(Cr)-N$(CH_2PO_3H_2)_2$ are shown in Figure 7. Two declining stages were observed for MIL-101(Cr)-N$(CH_2PO_3H_2)_2$ in the TG pattern. The amount of weight loss is estimated to be 5−7%, which can be attributed to the decreases in solvent (organic and water). The results show that the catalyst can be used up to 220 °C, which can be related to the departure of PO_3H_2 arms and decomposition of the structure of MIL-101(Cr)-N$(CH_2PO_3H_2)_2$ (Figure 7).

Nitrogen adsorption−desorption isotherms of MIL-101(Cr)-NH_2 and MIL-101(Cr)-N$(CH_2PO_3H_2)_2$ were measured and the results are presented in Figure 8a,c. Observation of hysteresis

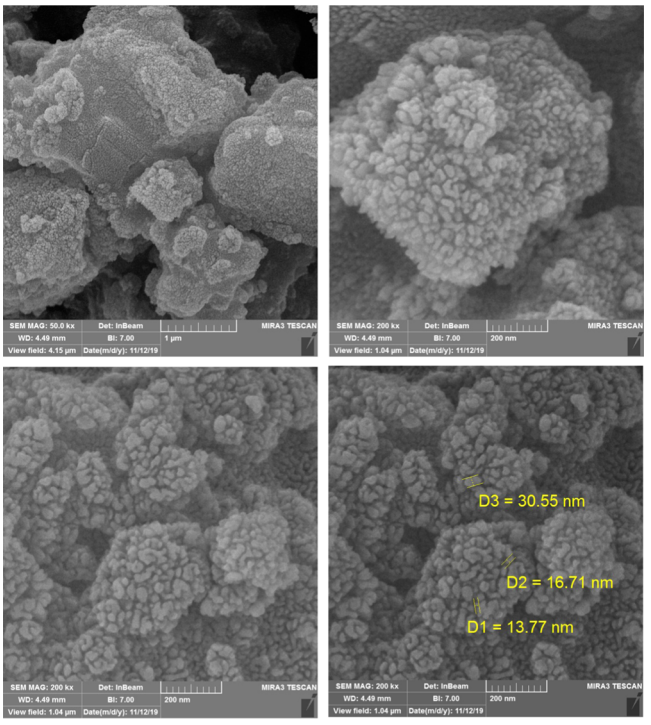

Figure 5. SEM images of MIL-101(Cr)-N$(CH_2PO_3H_2)_2$.

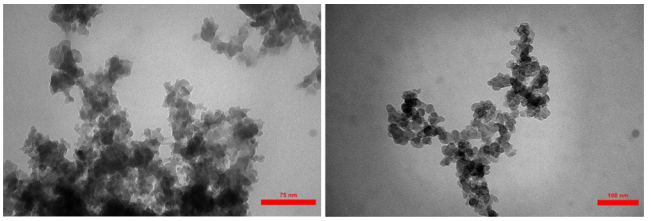

Figure 6. TEM of MIL-101(Cr)-N$(CH_2PO_3H_2)_2$.

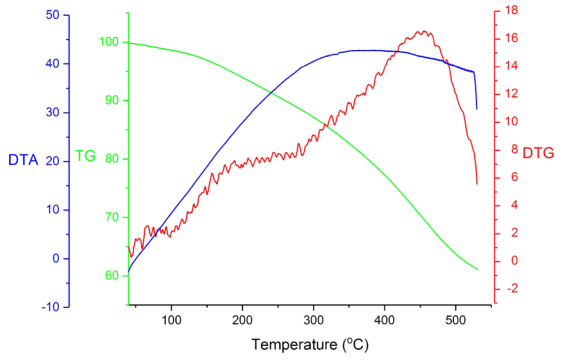

Figure 7. TG analysis, DTG analysis, and DTA of MIL-101(Cr)-N$(CH_2PO_3H_2)_2$.

loops for both of them means that the prepared catalysts are mesoporous. The obtained BET surface areas of MIL-101(Cr)-NH_2 and MIL-101(Cr)-N$(CH_2PO_3H_2)_2$ are 1708 and 528 m^2 g^{-1}, respectively. Their total pore volumes are 1.46 and 0.38 cm^3 g^{-1}, respectively. The Barrett−Joyner−Halenda (BJH) pore size distribution data are presented in Figure 8b,d, showing that most of the pores for both samples are smaller than 10 nm.

After the structure of MIL-101(Cr)-N$(CH_2PO_3H_2)_2$ was approved, it was used as a MOFs catalyst for the synthesis of *N*-amino-2-pyridones and pyrano [2,3-*c*]pyrazoles. To synthesi-

https://dx.doi.org/10.1021/acsomega.9b02133
ACS Omega 2020, 5, 6240−6249

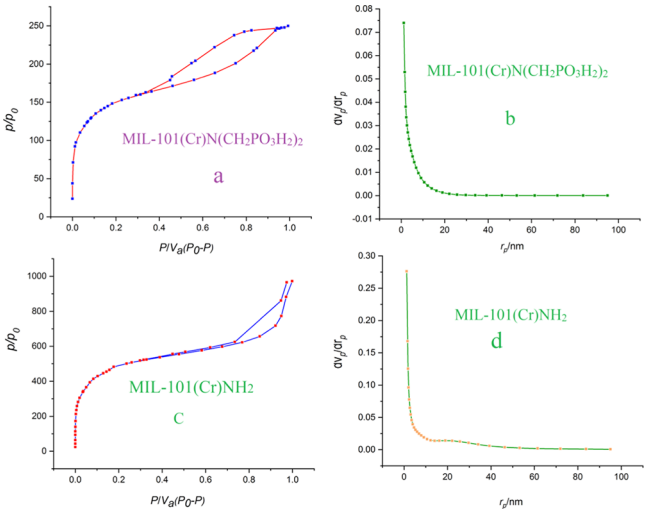

Figure 8. N_2 adsorption/desorption isotherm for (a) MIL-101(Cr)-NH_2 and (c) IL-101(Cr)-$N(CH_2PO_3H_2)_2$. (b, d) Their pore size distribution plots.

ze*N*-amino-2-pyridones, the four-part reaction between ethyl cyanoacetate (1 mmol, 0.113 g), hydrazine hydrate (1.2 mmol, 0.060 g), malononitrile (1.1 mmol, 0.072 g) and benzaldehyde (1 mmol, 0.106 g) under refluxing solvents such as: water, ethanol, acetonitrile, *n*-hexane solvents and solvent-free in the presence a catalytic amount of MIL-101(Cr)-$N(CH_2PO_3H_2)_2$ was tested, the results of which are shown in Table 1. The results are summarized in Table 1. The results show that refluxing water is best of choice for producing *N*-amino-2-pyridones (Table 1, entry 1). Increasing the amount of catalyst did not show any increase in efficiency (Table 1, entry 9). By decreasing the amounts of catalysts, a decrease in efficiency was observed (Table 1, entries 7 and 8). Reducing the temperature has increased the reaction time and reduced the efficiency of the product (Table 1, entries 10−13).

Table 1. Effect of Different Amounts of Catalysts, Temperature, and Solvent (5 mL) in the Synthesis of *N*-Amino-2-pyridones

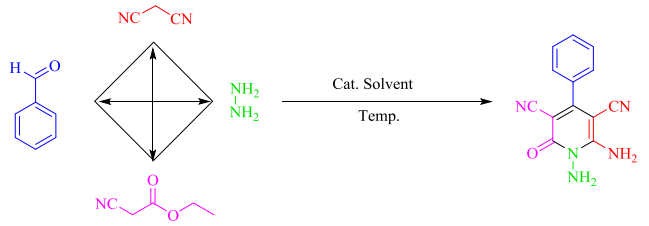

entry	catalysts (mg)	temperature (°C)	solvent	time (min)	yield (%)
1	10	reflux	H_2O	40	90
2	10	reflux	EtOH	60	72
3	10	reflux	*n*-hexane	90	trace
4	10	reflux	CH_3CN	45	76
5	10	110	toluene	65	55
6	10	100	solvent-free	60	43
7	7	80	H_2O	50	81
8	5	reflux	H_2O	60	80
9	15	reflux	H_2O	40	90
10	10	75	H_2O	55	78
11	10	50	H_2O	65	66
12	10	r.t.	H_2O	85	35
13		r.t.	H_2O	120	trace

After optimization of the reaction conditions for the synthesis of *N*-amino-2-pyridones, a wide range of aromatic aldehydes, including electron withdrawal, electron release and heterocyclic rings have been synthesized (Table 2). Then, to investigate the effect of the functional group, ethyl acetoacetate replaced ethyl cyanoacetate, and it was observed that the product of pyrano [2,3-*c*]pyrazoles was synthesized by changing the cyano group to the carbonyl group. Under optimal conditions for *N*-amino-2-pyridones, a wide range of pyrano [2,3-*c*]pyrazoles were also synthesized (Table 3). The results reveal that the described catalyst can produce *N*-amino-2-pyridones and pyrano [2,3-*c*]pyrazoles derivatives in short reaction time and high efficiency.

Alabugin has recently comprehensively reviewed the stereoelectronic effects as a bridge between structure and reactivity.[41−43] On the basis of Alabugin's concept, we have recently introduced a new term "vinylogous anomeric-based oxidation".[44−48] Vinylogous anomeric effect has been approved by Katritzky.[49] In the cooperative vinylogous anomeric-based oxidation mechanism, through a multicomponent reaction strategy, starting materials interact with each other to yield a suitable intermediate. The vinylogous anomeric effect is the major driving force of oxidation and/or aromatization of intermediate for preparing the desired product. For example, in the case of 2-amino-4,6-diphenylnicotinonitrile a cooperative vinylogous anomeric-based oxidation mechanism occurs at the related intermediate (Scheme 3).[50] A wide range of aromatized molecules through the described mechanism have been reported.[51]

The anomeric effect can lead to bond weakening in a wide range of organic reactions. For example, recently we have suggested that in the Cannizzaro reaction after the addition of hydroxide (OH^-) to the carbonyl group of aldehydes which did not have α-hydrogen (Scheme 4), both the lone pairs of electrons of oxygen atoms within the tetrahedral carbon shared their electrons in the antibonding orbital of the C−H bond ($n_N \rightarrow \sigma^*_{C-H}$) and weakened it. The resulting labile hydride acts as a powerful nucleophile that attacks the second molecule of aldehyde. Finally, this reaction produced equal amounts of corresponding alcohol and acid.[52]

On the basis of the above-mentioned background, a rational mechanism for the synthesis of *N*-amino-2-pyridones based on a cooperative vinylogous anomeric-based oxidation for the final step is suggested in Scheme 5. At first, the carbonyl group of aldehyde is activated by the acidic group of MIL-101(Cr)-$N(CH_2PO_3H_2)_2$. Malononitrile reacts with the carbonyl group of aldehyde to afford an intermediate **I** by removing one molecule of H_2O. Then, compound (A) attacks intermediate **I** as a Michael acceptor to give intermediate **II**. Further, intermediate **II** with intramolecular cyclocondensation reacts to give **III**. Finally, intermediate **III** was derived via a cooperative vinylogous anomeric-based oxidation ($-H_2$) to give the desired product (Scheme 5). It should be noted that the target reaction was also carried out under argon and nitrogen atmospheres to make sure that the final desired product was not produced via an aerobic oxidation pathway. The reaction was performed successfully under the air atmosphere. Thus, our evidence shows that the target reaction was preceded via a cooperative vinylogous anomeric-based oxidation mechanism.

To evaluate the performance of MIL-101(Cr)-N-$(CH_2PO_3H_2)_2$ as a catalyst for the preparation of *N*-amino-2-pyridones, we have used various organic and inorganic acid

https://dx.doi.org/10.1021/acsomega.9b02133
ACS Omega 2020, 5, 6240−6249

Table 2. Synthesis of *N*-Amino-2-pyridones Using MIL-101(Cr)-N($CH_2PO_3H_2$)$_2$

Entry	Product	Time (min)	Yield (%)	M. p (°C) Found (Lit. [Ref.])
1	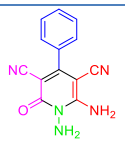 6a	40	88	237-240 (237-239) [22]
2	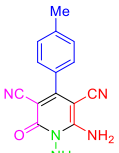 6b	35	90	240-241 (238–240) [22]
3	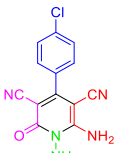 6c	25	91	341-342 (340) [23]
4	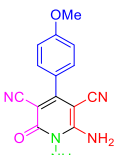 6d	35	90	(222-224) 222-224 [22]
5	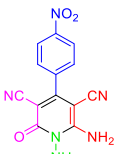 6e	20	92	>340 (360) [23]
6	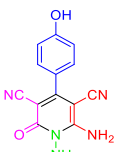 6f	25	90	325-327
7	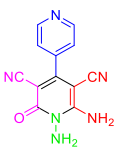 6g	25	85	337-339
8	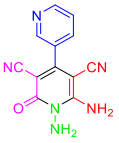 6h	25	87	311-312 (310-312)[30]
9	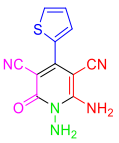 6i	30	86	300 (297 – 298)[30]
10	 6j	35	74	325-327
11	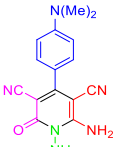 6k	25	89	249-251 (250) [31]
12	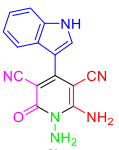 6l	30	88	>350
13	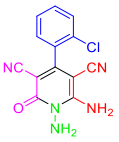 6m	25	87	305-306 (305-307)[23]
14	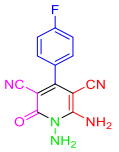 6n	30	85	337(338-340)[32]
15	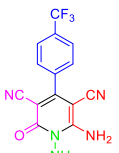 6o	25	90	>340 (365)[32]

catalysts for the condensation reaction between 4-nitro benzaldehyde (1 mmol, 0.151 g), ethyl cyanoacetate (1 mmol, 0.113 g), hydrazine hydrate (1.2 mmol, 0.060 g), and malononitrile (1.1 mmol, 0.072 g) (Table 3). As indicated in Table 3, MIL-101(Cr)-N($CH_2PO_3H_2$)$_2$ is the best catalyst for the synthesis of *N*-amino-2-pyridone derivatives (Table 4).

According to the results in Figure 9, MIL-101(Cr)-N($CH_2PO_3H_2$)$_2$ can be separated by centrifugation and reused without significantly reducing its catalytic activity. For this purpose, recyclability of the catalyst was tested in the reaction between 4-nitro benzaldehyde (1 mmol, 0.151 g), ethyl cyanoacetate (1 mmol, 0.113 g), hydrazine hydrate (1.2 mmol, 0.060 g), and malononitrile (1.1 mmol, 0.072 g) as a model reaction under the above-mentioned optimized reaction conditions. Therefore, MIL-101(Cr)-N($CH_2PO_3H_2$)$_2$ can be reused up to six runs without noticeable changes in the catalytic activity.

https://dx.doi.org/10.1021/acsomega.9b02133
ACS Omega 2020, 5, 6240−6249

Table 3. Synthesis of Pyrano [2,3-*c*]pyrazoles Using MIL-101(Cr)-N($CH_2PO_3H_2$)$_2$

Entry	Product	Time (min)	Yield (%)	M. p (°C) Found (Lit. [Ref.])
1	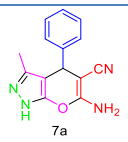 7a	25	90	243-245 (243 – 246) [33]
2	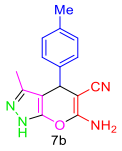 7b	22	89	195-196 (196-198) [34]
3	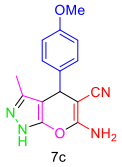 7c	25	91	210-212 (210-213) [35]
4	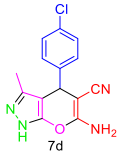 7d	20	90	232-235(231– 235) [35]
5	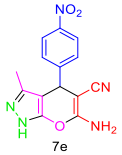 7e	15	93	251-253(250-252) [36]
6	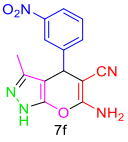 7f	20	91	213-215(214-216) [35]
7	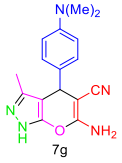 7g	25	76	168-170(168-170) [33]
8	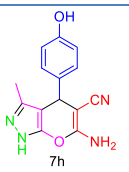 7h	30	84	225-227(224-226) [33]
9	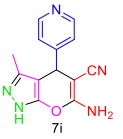 7i	20	87	215-217(215-217) [37]
10	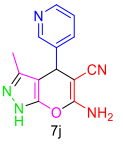 7j	20	88	215-216 (216-217)[38]
11	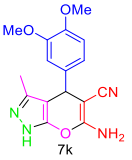 7k	25	85	193(192-194)[39]
12	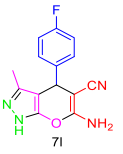 7l	20	86	243(242-244)[40]
13	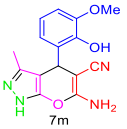 7m	25	81	228-230(240-242)

Scheme 3. Cooperative Vinylogous Anomeric-Based Oxidation Leads to the Production of 2-Amino-4,6-diphenylnicotinonitrile

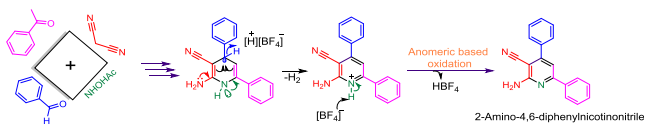

Scheme 4. Anomeric-Based Oxidation Leads to Hydride Transfer in the Mechanism of Cannizzaro Reaction

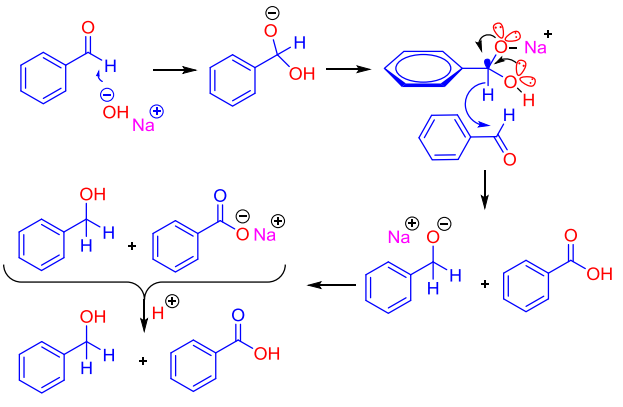

3. CONCLUSIONS

After the preparation of metal−organic framework MIL-101(Cr)-NH_2 with phosphorous acid functional groups, its structure was approved. The presented MIL-101(Cr)-N-($CH_2PO_3H_2$)$_2$ was successfully applied for producing a wide range of pyrano [2,3-*c*]pyrazole and *N*-amino-2-pyridone derivatives via cooperative vinylogous anomeric-based oxidation mechanism. Short reaction times, clean profile of reaction, easy

https://dx.doi.org/10.1021/acsomega.9b02133
ACS Omega 2020, 5, 6240−6249

Scheme 5. Proposed Mechanism for the Synthesis *N*-Amino-2-pyridones Using MIL-101(Cr)-N($CH_2PO_3H_2$)$_2$

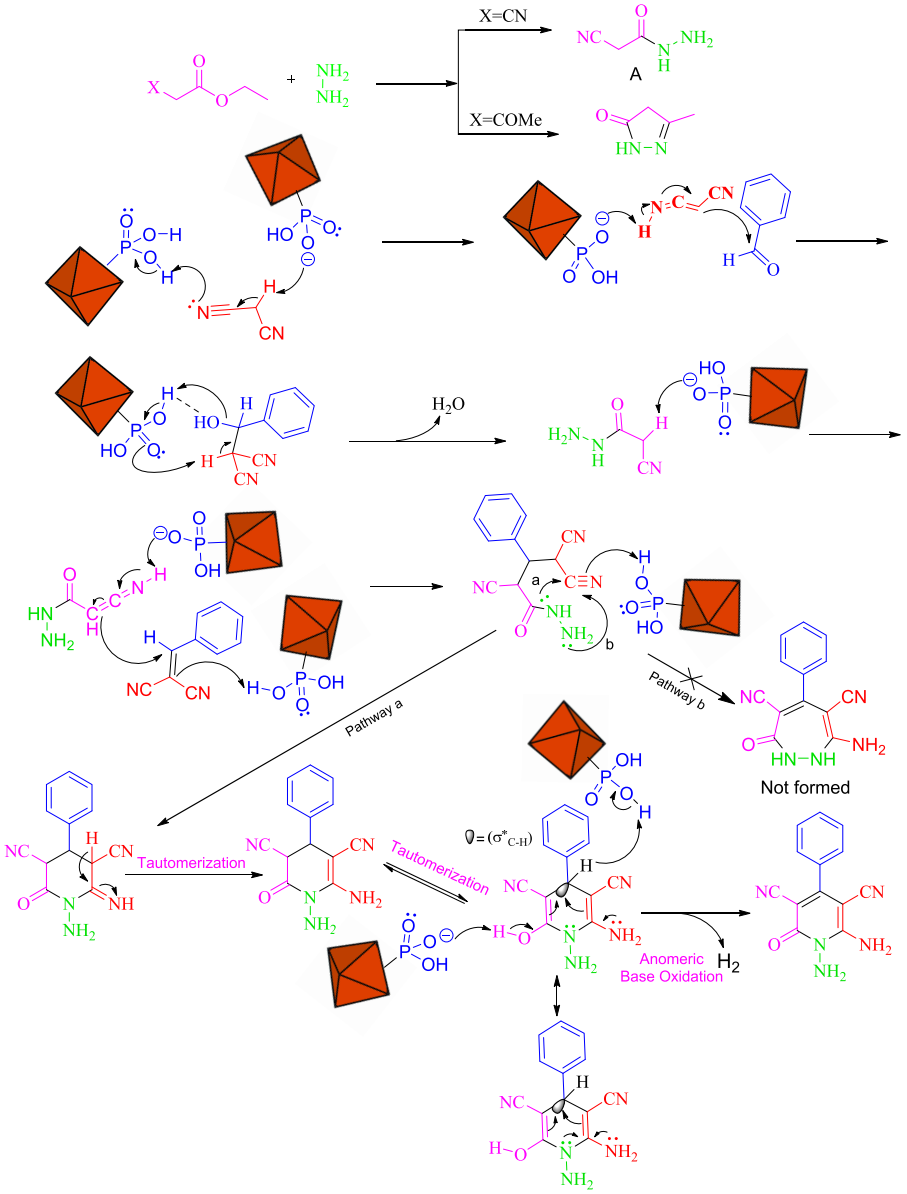

work-up, recyclability, and reusability of catalyst are advantages of the presented methodology.

4. EXPERIMENTAL SECTION

4.1. General Procedure for the Preparation of MIL-101(Cr)-NH_2. MIL-101(Cr)-NH_2 was synthesized according to our previously reported experimental procedure.[28,29] A mixture of $Cr(NO_3)_3{\cdot}9(H_2O)$ (2 mmol, 0.8 g), 2-aminoterephthalic acid (2 mmol, 0.362 g), and sodium hydroxide (5 mmol, 0.2 g) was dispersed and then stirred in 20 mL of water for 10 min. The resulting solution was heated in a Teflon-lined autoclave at 150 °C for 12 h. After cooling the reaction mixture to room temperature, the green solid was collected, washed with dimethylformamide (DMF), and then further purified by solvothermal treatment in ethanol at 100 °C for 24 h. Finally, the desired product was dried at 80 °C in a vacuum oven.

4.2. General Procedure for the Preparation of MIL-101(Cr)-N($CH_2PO_3H_2$)$_2$. In a 50 mL round-bottom flask, MIL-101(Cr)-NH_2 (1 g), formaldehyde (0.33 mL, 9 mmol), phosphorus acid (0.665 mL, 9 mmol), *p*-TSA (10 mol %, 0.017 g), and ethanol (25 mL) were refluxed for 8 h. Then, it was washed three times with ethanol and dried in a vacuum oven at 70 °C to obtain MIL-101(Cr)-N($CH_2PO_3H_2$)$_2$ (1.7 g) (Scheme 6). The amount of phosphorus is 4.56% of the MOFs component of MIL-101(Cr)-N($CH_2PO_3H_2$)$_2$.

4.3. General Procedure for the Synthesis of Pyrano [2,3-*c*]pyrazole and *N*-Amino-2-pyridone Derivatives (10a−10t) Using MIL-101(Cr)-N($CH_2PO_3H_2$)$_2$. In a four-component reaction in water reflux conditions, including ethyl cyanoacetate or ethyl acetoacetate (1 mmol), hydrazine hydrate (1.2 mmol, 0.060 g), malononitrile (1.1 mmol, 0.072 g), aldehyde (1 mmol), and MIL-101(Cr)-N($CH_2PO_3H_2$)$_2$ (10 mg) were stirred in a 25 mL round-bottom flask (time for any case has been presented in Tables 2 and 3). Thin-layer chromatography (TLC) technique was used to assess the reaction progress. After the reaction was completed, the solvent was evaporated and then 2 mL of ethylene glycol was added to the reaction mixture. The catalyst was removed from the

https://dx.doi.org/10.1021/acsomega.9b02133
ACS Omega 2020, 5, 6240−6249

Table 4. Evaluation of Various Catalysts for the Synthesis of *N*-Amino-2-pyridones in Comparison with MIL-101(Cr)-$N(CH_2PO_3H_2)_2$ in Ethanol under Reflux Conditions

entry	catalyst	amount of catalyst (mol %)	time (min)	yield (%)
1	MIL-101(Cr)-$N(CH_2PO_3H_2)_2$	5 mg	20	92
2	MIL-101(Cr)-NH_2	5 mg	60	24
3	$[Py\text{-}SO_3H]Cl$[53]	10	35	82
4	$Fe_3O_4@SiO_2@PrNH_2$[54]	5 mg	60	25
5	SSA[55]	10	25	85
6	TrBr	15	60	65
7	*p*-TSA	10	45	65
8	nano-SB-[PSIM]Cl[56]	10	35	78
9	TrCl	10	45	72
10	GTBSA[57]	10	30	85
11	$[Fe_3O_4@SiO_2@Pr\text{-}DABCO\text{-}SO_3H]Cl_2$[58]	10 mg	35	82
12	$FeCl_3$	10	50	75
13	$Al(HSO_4)_3$	10	45	75
14	$H_3[p(W_3O_{10})_4]\cdot xH_2O$	15	60	75
15	Fe_3O_4	10 mg	55	68
16	trichloroisocyanuric acid	10	55	70
17	Et_3N	20	60	trace
18	$NaHSO_4$	10	60	35
19	H_3PO_3	10	20	75
20	H_3PO_3 + MIL-101(Cr)-NH_2	5 + 5	20	90 and without recycling

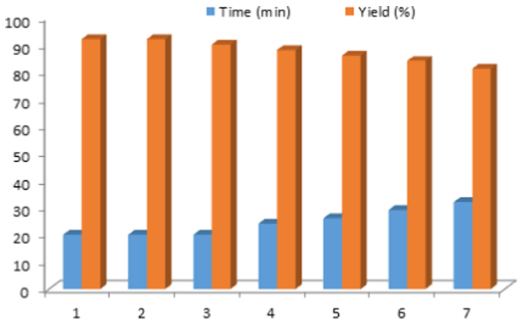

Figure 9. Recyclability of MIL-101(Cr)-$N(CH_2PO_3H_2)_2$ for the synthesis of *N*-amino-2-pyridone compounds.

Scheme 6. Synthesis of MIL-101(Cr)-$N(CH_2PO_3H_2)_2$ Containing Phosphorous Acid Groups

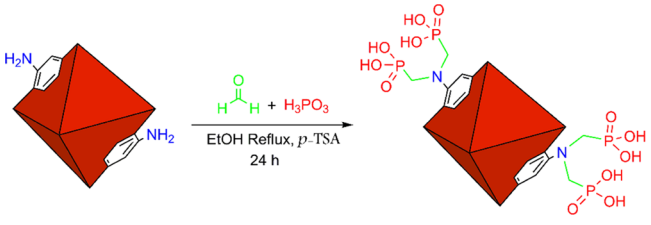

reaction using centrifugation at 1000 rpm. The product was purified using 96% ethanol (Scheme 2).

■ ASSOCIATED CONTENT

Supporting Information

The Supporting Information is available free of charge at https://pubs.acs.org/doi/10.1021/acsomega.9b02133.

FT-IR; ^1H NMR; and ^{13}C NMR spectroscopy details (PDF)

■ AUTHOR INFORMATION

Corresponding Authors

Mahmoud Zarei − *Department of Organic Chemistry, Faculty of Chemistry, Bu-Ali Sina University, Hamedan, Iran;* orcid.org/0000-0002-3701-9755; Phone: +988138282807; Email: mahmoud8103@yahoo.com; Fax: +988138380709

Mohammad Ali Zolfigol − *Department of Organic Chemistry, Faculty of Chemistry, Bu-Ali Sina University, Hamedan, Iran;* orcid.org/0000-0002-4970-8646; Email: zolfi@basu.ac.ir, mzolfigol@yahoo.com

Sadegh Rostamnia − *Organic and Nano Group (ONG), Department of Chemistry, Faculty of Science, University of Maragheh, Maragheh, Iran;* orcid.org/0000-0001-6310-8754; Email: srostamnia@gmail.com

Authors

Saeed Babaee − *Department of Organic Chemistry, Faculty of Chemistry, Bu-Ali Sina University, Hamedan, Iran*

Hassan Sepehrmansourie − *Department of Organic Chemistry, Faculty of Chemistry, Bu-Ali Sina University, Hamedan, Iran*

Complete contact information is available at: https://pubs.acs.org/10.1021/acsomega.9b02133

Notes

The authors declare no competing financial interest.

■ ACKNOWLEDGMENTS

We thank the Bu-Ali Sina University and Iran National Science Foundation (INSF) (Grant No. 98001912) for financial support.

■ REFERENCES

(1) Li, H.; Eddaoudi, M.; O'Keeffe, M.; Yaghi, O. M. Design and synthesis of an exceptionally stable and highly porous metal−organic framework. *Nature* **1999**, *402*, 276−279.

(2) Lee, J. Y.; Farha, O. K.; Roberts, J.; Scheidt, K. A.; Nguyen, S. T.; Hupp, J. T. Metal−organic framework materials as catalysts. *Chem. Soc. Rev.* **2009**, *38*, 1450−1459.

(3) Goetjen, T. A.; Zhang, X.; Liu, J.; Hupp, J. T.; Farha, O. K. Metal−Organic Framework supported single site chromium (III) catalyst for ethylene oligomerization at low pressure and temperature. *ACS Sustainable Chem. Eng.* **2019**, *7*, 2553−2557.

(4) Nowacka, A. E.; Briantais, P.; Prestipino, C.; Llabrés i Xamena, F. X. Selective aerobic oxidation of cumene to cumene hydroperoxide over mono-and bimetallic trimesate metal−organic frameworks prepared by a facile "green" aqueous synthesis. *ACS Sustainable Chem. Eng.* **2019**, *7*, 7708−7715.

(5) Cao, C.-C.; Chen, C.-X.; Wei, Z.-W.; Qiu, Q.-F.; Zhu, N.-X.; Xiong, Y.-Y.; Jiang, J.-J.; Wang, D.; Su, C.-Y. Catalysis through dynamic spacer installation of multivariate functionalities in metal−organic frameworks. *J. Am. Chem. Soc.* **2019**, *141*, 2589−2593.

(6) Huang, X. C.; Lin, Y. Y.; Zhang, J. P.; Chen, X. M. Ligand-directed strategy for zeolite-type metal−organic frameworks: zinc (II) imidazolates with unusual zeolitic topologies. *Angew. Chem., Int. Ed.* **2006**, *45*, 1557−1559.

(7) Doustkhah, E.; Lin, J.; Rostamnia, S.; Len, C.; Luque, R.; Luo, X.; Bando, Y.; Wu, K. C. W.; Kim, J.; Yamauchi, Y.; Ide, Y. Development of sulfonic-acid-functionalized mesoporous materials: synthesis and catalytic applications. *Chem. - Eur. J.* **2019**, *25*, 1614−1635.

(8) Alamgholiloo, H.; Rostamnia, S.; Hassankhani, A.; Banaei, R. Synthesis of a zeolitic imidazolate−zinc metal−organic framework and

https://dx.doi.org/10.1021/acsomega.9b02133
ACS Omega 2020, 5, 6240−6249

the combination of its catalytic properties with 2, 2, 2-trifluoroethanol for *N*-formylation. *Synlett* **2018**, *26*, 1593−1596.
(9) Jhung, S. H.; Khan, N. A.; Hasan, Z. Analogous porous metal−organic frameworks: synthesis, stability and application in adsorption. *CrystEngComm* **2012**, *14*, 7099−7109.
(10) Yang, C.-X.; Yan, X.-P. Metal−organic framework MIL-101 (Cr) for high-performance liquid chromatographic separation of substituted aromatics. *Anal. Chem.* **2011**, *83*, 7144−7150.
(11) Mitsunobu, O.; Yamada, M. Preparation of esters of carboxylic and phosphoric acid via quaternary phosphonium salts. *Bull. Chem. Soc. Jpn.* **1967**, *40*, 2380−2382.
(12) Jalili, F.; Zarei, M.; Zolfigol, M. A.; Rostamnia, S.; Moosavi-Zare, A. R. SBA-15/PrN $(CH_2PO_3H_2)_2$ as a novel and efficient mesoporous solid acid catalyst with phosphorous acid tags and its application on the synthesis of new pyrimido [4, 5-*b*] quinolones and pyrido [2, 3-d] pyrimidines via anomeric based oxidation. *Microporous Mesoporous Mater.* **2019**, *294*, No. 109865.
(13) Afsar, J.; Zolfigol, M. A.; Khazaei, A.; Zarei, M.; Gu, Y.; Alonso, D. A.; Khoshnood, A. Synthesis and application of melamine-based nano catalyst with phosphonic acid tags in the synthesis of (3′-indolyl) pyrazolo [3, 4-*b*] pyridines via vinylogous anomeric based oxidation. *Mol. Catal.* **2019**, *482*, No. 110666.
(14) Sepehrmansouri, H.; Zarei, M.; Zolfigol, M. A.; Moosavi-Zare, A. R.; Rostamnia, S.; Moradi, S. Multilinker phosphorous acid anchored En/MIL-100 (Cr) as a novel nanoporous catalyst for the synthesis of new *N*-heterocyclic pyrimido [4, 5-*b*] quinolines. *Mol. Catal.* **2019**, *481*, No. 110303.
(15) Zarei, M.; Zolfigol, M. A.; Moosavi-Zare, A. R.; Noroozizadeh, E.; Rostamnia, S. Three-Component Synthesis of Spiropyrans Using SBA-15/En Bonded Phosphorous Acid [SBA-15/Pr-NH_{1-y} $(CH_2PO_3H_2)$y-Et-NH_{2-x} $(CH_2PO_3H_2)_x$] as a New Nanoporous Heterogeneous Catalyst. *ChemistrySelect* **2018**, *3*, 12144−12149.
(16) Moradi, S.; Zolfigol, M. A.; Zarei, M.; Alonso, D. A.; Khoshnood, A. Synthesis of a Biological-Based Glycoluril with Phosphorous Acid Tags as a New Nanostructured Catalyst: Application for the Synthesis of Novel Natural Henna-Based Compounds. *ChemistrySelect* **2018**, *3*, 3042−3047.
(17) Dalvie, D. K.; Kalgutkar, A. S.; Khojasteh-Bakht, S. C.; Obach, R. S.; O'Donnell, J. P. Biotransformation Reactions of Five-Membered Aromatic Heterocyclic Rings. *Chem. Res. Toxicol.* **2002**, *15*, 269−299.
(18) Mikhailopulo, I. A.; Poopeiko, N.; Prikota, T.; Sivets, G.; Kvasyuk, E. I.; Balzarini, J.; De Clercq, E. Synthesis and antiviral and cytostatic properties of 3′-deoxy-3′-fluoro-and 2′-azido-3′-fluoro-2′, 3′-dideoxy-D-ribofuranosides of natural heterocyclic bases. *J. Med. Chem.* **1991**, *34*, 2195−2202.
(19) Tietze, L. F.; Rackelmann, N. Domino reactions in the synthesis of heterocyclic natural products and analogs. *Pure Appl. Chem.* **2004**, *76*, 1967−1983.
(20) Johnson, L. E.; Dietz, A. Kalafungin, a new antibiotic produced by Streptomyces tanashiensis strain Kala. *Appl. Environ. Microbiol.* **1968**, *16*, 1815−1821.
(21) Zheng, H.; Li, L.; Sun, B.; Gao, Y.; Song, W.; Zhao, X.; Gao, Y.; Xie, Z.; Zhang, N.; Ji, J.; Yuan, H.; Lou, H. Design and synthesis of furyl/thineyl pyrroloquinolones based on natural alkaloid perlolyrine, lead to the discovery of potent and selective PDE5 inhibitors. *Eur. J. Med. Chem.* **2018**, *150*, 30−38.
(22) Safaei-Ghomi, J.; Saberimoghadam, M. R.; Shahbazialavi, H.; Asgarikheirabadi, M. An efficient method for the synthesis of *N*-amino-2-pyridones using reusable catalyst ZnO nanoparticles. *J. Chem. Res.* **2014**, *38*, 583−585.
(23) Hosseini, H.; Bayat, M. An efficient and ecofriendly synthesis of highly functionalized pyridones via a one-pot three-component reaction. *RSC Adv.* **2018**, *8*, 27131−27143.
(24) Safaei-Ghomia, J.; Asgari-Kheirabadia, M.; Shahbazi-Alavia, H.; Ziaratib, A. Synthesis of methyl 6-amino-5-cyano-4-aryl-2, 4-dihydropyrano [2, 3-*c*] pyrazole-3-carboxylates using nano-$ZnZr_4(PO_4)_6$ as an efficient catalyst. *Iran. J. Catal.* **2016**, *6*, 319−324.
(25) Kiyani, H.; Bamdad, M. Sodium ascorbate as an expedient catalyst for green synthesis of polysubstituted 5-aminopyrazole-4-carbonitriles and 6-amino-1, 4-dihydropyrano [2, 3-*c*] pyrazole-5-carbonitriles. *Res. Chem. Intermed.* **2018**, *44*, 2761−2778.
(26) Jagodić, V. Infrared Spectra of Organophosphorus Compounds. III. *Croat. Chem. Acta* **1977**, *49*, 127−133.
(27) Zhou, M.; Andrews, L. Infrared spectra and density functional calculations of the CrO_2^-, MoO_2^-, and WO_2^- molecular anions in solid neon. *J. Chem. Phys.* **1999**, *111*, 4230−4238.
(28) Férey, G.; Mellot-Draznieks, C.; Serre, C.; Millange, F.; Dutour, J.; Surblé, S.; Margiolaki, I. A chromium terephthalate-based solid with unusually large pore volumes and surface area. *Science* **2005**, *309*, 2040−2042.
(29) Rostamnia, S.; Alamgholiloo, H.; Jafari, M. Ethylene diamine post-synthesis modification on open metal site Cr-MOF to access efficient bifunctional catalyst for the Hantzsch condensation reaction. *Appl. Organomet. Chem.* **2018**, *32*, No. e4370.
(30) Abdel Latif, F. F.; Mekheimer, R.; Ahmed, E. K.; Abdel Aleem, T. A simple route for the synthesis of pyrano [2, 3-*c*] pyrazole and pyridine-2-one derivatives. *Pharmazie* **1993**, *48*, 736−738.
(31) Soto, J. L.; Seoane, C.; Zamorano, P.; Cuadrado, F. J. A convenient synthesis of *N*-amino-2-pyridones. *Synthesis* **1981**, *1981*, 529−530.
(32) Assiria, M. A.; Abdel-Kariemc, S. M.; Alic, T. E.; Yahiad, I. The Free Internet Journal for Organic Chemistry. *Org. Chem.* **2018**, 240−253.
(33) Upadhyay, A.; Sharma, L. K.; Singh, V. K.; Dubey, R.; Kumar, N.; Singh, R. K. P. Electrochemically induced one pot synthesis of 1, 4-dihydropyrano [2, 3-*c*]-pyrazole-5-carbonitrile derivatives via a four component-tandem strategy. *Tetrahedron Lett.* **2017**, *58*, 1245−1249.
(34) Maleki, B.; Eshghi, H.; Barghamadi, M.; Nasiri, N.; Khojastehnezhad, A.; Ashrafi, S. S.; Pourshiani, O. Silica-coated magnetic $NiFe_2O_4$ nanoparticles-supported $H_3PW_{12}O_{40}$; synthesis, preparation, and application as an efficient, magnetic, green catalyst for one-pot synthesis of tetrahydrobenzo [*b*] pyran and pyrano [2, 3-*c*] pyrazole derivatives. *Res. Chem. Intermed.* **2016**, *42*, 3071−3093.
(35) Survase, D.; Bandgar, B.; Helavi, V. Polyethylene glycol-promoted synthesis of pyrimido [1, 2-*a*] benzimidazole and pyrano [2, 3-*c*] pyrazole derivatives in water. *Synth. Commun.* **2017**, *47*, 680−687.
(36) Safaei-Ghomi, J.; Shahbazi-Alavi, H.; Heidari-Baghbahadorani, E. $ZnFe_2O_4$ nanoparticles as a robust and reusable magnetically catalyst in the four component synthesis of [(5-hydroxy-3-methyl-1*H*-pyrazol-4yl)(phenyl) methyl] propanedinitriles and substituted 6-amino-pyrano [2, 3-*c*] pyrazoles. *J. Chem. Res.* **2015**, *39*, 410−413.
(37) Bakherad, M.; Keivanloo, A.; Gholizadeh, M.; Doosti, R.; Javanmardi, M. Using magnetized water as a solvent for a green, catalyst-free, and efficient protocol for the synthesis of pyrano [2, 3-c] pyrazoles and pyrano [4′, 3′: 5, 6] pyrazolo [2, 3-d] pyrimidines. *Res. Chem. Intermed.* **2017**, *43*, 1013−1029.
(38) Kamel, M. M. Convenient synthesis, characterization, cytotoxicity and toxicity of pyrazole derivatives. *Acta Chim. Slov.* **2015**, *62*, 136−141.
(39) Shaterian, H. R.; Azizi, K. Mild, four-component synthesis of 6-amino-4-aryl-3-methyl-1, 4-dihydropyrano [2, 3-*c*] pyrazole-5-carbonitriles catalyzed by titanium dioxide nano-sized particles. *Res. Chem. Intermed.* **2014**, *40*, 661−667.
(40) Vekariya, R. H.; Patel, K. D.; Patel, H. D. Fruit juice of Citrus limon as a biodegradable and reusable catalyst for facile, eco-friendly and green synthesis of 3, 4-disubstituted isoxazol-5 (4*H*)-ones and dihydropyrano [2, 3-*c*]-pyrazole derivatives. *Res. Chem. Intermed.* **2016**, *42*, 7559−7579.
(41) Alabugin, I. V. *Stereoelectronic Effects: A Bridge between Structure and Reactivity*; John Wiley & Sons, 2016.
(42) Alabugin, I. V.; dos Passos Gomes, G.; Abdo, M. A. Hyperconjugation. *WIREs Comput. Mol. Sci.* **2019**, *9*, No. e1389.
(43) Alabugin, I. V.; Gilmore, K. M.; Peterson, P. W. Hyperconjugation. *WIREs Comput. Mol. Sci.* **2011**, *1*, 109−141.
(44) Torabi, M.; Yarie, M.; Zolfigol, M. A. Synthesis of a novel and reusable biological urea based acidic nanomagnetic catalyst: Application for the synthesis of 2-amino-3-cyano pyridines via cooperative

https://dx.doi.org/10.1021/acsomega.9b02133
ACS Omega 2020, 5, 6240−6249

vinylogous anomeric based oxidation. *Appl. Organomet. Chem.* **2019**, *33*, No. e4933.
(45) Karimi, F.; Zolfigol, M. A.; Yarie, M. A novel and reusable ionically tagged nanomagnetic catalyst: Application for the preparation of 2-amino-6-(2-oxo-2*H*-chromen-3-yl)-4-arylnicotinonitriles via vinylogous anomeric based oxidation. *Mol. Catal.* **2019**, *463*, 20−29.
(46) Noura, S.; Ghorbani, M.; Zolfigol, M. A.; Narimani, M.; Yarie, M.; Oftadeh, M. Biological based (nano) gelatoric ionic liquids (NGILs): Application as catalysts in the synthesis of a substituted pyrazole via vinylogous anomeric based oxidation. *J. Mol. Liq.* **2018**, *271*, 778−785.
(47) Zolfigol, M. A.; Kiafar, M.; Yarie, M.; Taherpour, A. A.; Fellowes, T.; Hancok, A. N.; Yari, A. A convenient method for preparation of 2-amino-4, 6-diphenylnicotinonitrile using HBF_4 as an efficient catalyst via an anomeric based oxidation: A joint experimental and theoretical study. *J. Mol. Struct.* **2017**, *1137*, 674−680.
(48) Babaee, S.; Zolfigol, M. A.; Zarei, M.; Zamanian, J. 1, 10-Phenanthroline-Based Molten Salt as a Bifunctional Sulfonic Acid Catalyst: Application to the Synthesis of *N*-Heterocycle Compounds via Anomeric Based Oxidation. *ChemistrySelect* **2018**, *3*, 8947−8954.
(49) Katritzky, A. R.; Steel, P. J.; Denisenko, S. N. X-Ray crystallographic evidence for a vinylogous anomeric effect in benzotriazole-substituted heterocycles. *Tetrahedron* **2001**, *57*, 3309−3314.
(50) Kalhor, S.; Yarie, M.; Rezaeivala, M.; Zolfigol, M. A. Novel magnetic nanoparticles with morpholine tags as multirole catalyst for synthesis of hexahydroquinolines and 2-amino-4, 6-diphenylnicotinonitriles through vinylogous anomeric-based oxidation. *Res. Chem. Intermed.* **2019**, *45*, 3453−3480.
(51) Yarie, M. Catalytic anomeric based oxidation. *Iran. J. Catal.* **2017**, *7*, 85−88.
(52) Kiafar, M.; Zolfigol, M. A.; Yarie, M.; Taherpour, A. The first computational study for the oxidative aromatization of pyrazolines and 1,4-dihydropyridines using 1,2,4-triazolinediones: an anomeric-based oxidation. *RSC Adv.* **2016**, *6*, 102280−102291.
(53) Moosavi-Zare, A. R.; Zolfigol, M. A.; Zarei, M.; Zare, A.; Khakyzadeh, V.; Hasaninejad, A. Design, characterization and application of new ionic liquid 1-sulfopyridinium chloride as an efficient catalyst for tandem Knoevenagel−Michael reaction of 3-methyl-1-phenyl-1H-pyrazol-5 (4*H*)-one with aldehydes. *Appl. Catal., A* **2013**, *467*, 61−68.
(54) Zolfigol, M. A.; Moosavi-Zare, A. R.; Zarei, M.; Zare, A.; Noroozizadeh, E.; Karamian, R.; Asadbegy, M. Synthesis of *β*-phthalimido-alcohols via regioselective ring opening of epoxide by using reusable basic magnetic nano particles and their biological investigation. *RSC Adv.* **2016**, *6*, 62460−62466.
(55) Zolfigol, M. A. Silica sulfuric acid/$NaNO_2$ as a novel heterogeneous system for production of thionitrites and disulfides under mild conditions. *Tetrahedron* **2001**, *57*, 9509−9511.
(56) Zare, A.; Merajoddin, M.; Moosavi-Zare, A. R.; Zarei, M.; Beyzavi, M. H.; Zolfigol, M. A. Design and characterization of nano-silica-bonded 3-n-propyl-1-sulfonic acid imidazolium chloride {nano-SB-[PSIM]Cl} as a novel, heterogeneous and reusable catalyst for the condensation of arylaldehydes with *β*-naphthol and alkyl carbamates. *Res. Chem. Intermed.* **2016**, *42*, 2365−2378.
(57) Zarei, M.; Sepehrmansourie, H.; Zolfigol, M. A.; Karamian, R.; Farida, S. H. M. Novel nano-size and crab-like biological-based glycoluril with sulfonic acid tags as a reusable catalyst: its application to the synthesis of new mono-and bis-spiropyrans and their in vitro biological studies. *New J. Chem.* **2018**, *42*, 14308−14317.
(58) Rajabi-Salek, M.; Zolfigol, M. A.; Zarei, M. Synthesis of a novel DABCO-based nanomagnetic catalyst with sulfonic acid tags: application to the synthesis of diverse spiropyrans. *Res. Chem. Intermed.* **2018**, *44*, 5255−5269.

https://dx.doi.org/10.1021/acsomega.9b02133
ACS Omega 2020, 5, 6240−6249